PCCP

ROYAL SOCIETY OF CHEMISTRY

PAPER

View Article Online
View Journal

Cite this: DOI: 10.1039/d5cp04724b

Picosecond time-resolved investigation of $NO_3^\bullet$ in PUREX solvent

Amel Zorai, *[a] Daniel Adjei, [a] Mireille Benoît, [a] Sergey Denisov, [a] Philippe Moisy, [b] Jacqueline Belloni [a] and Mehran Mostafavi *[a]

The early phenomena induced by the irradiation of solvents used in the PUREX process are investigated using picosecond electron pulse radiolysis. Various concentrations of solvent components – namely nitric acid (HNO_3), tributyl phosphate (TBP), dodecane, and, to a lesser extent, water are studied, in absence of the spent nuclear fuel. The transient optical absorption spectra at 5 ps constitute of the spectra of solvated electron in TBP and $NO_3^\bullet$ radical, characterized by absorption band with maxima at 640 nm and 670 nm, as well as a band at 440 nm. The yield of each species is determined. While the concentrations of HNO_3 and TBP of the environments exhibit opposing trends, the highest $NO_3^\bullet$ yield is recorded in a solution of 1.9 M HNO_3/3.3 M TBP/0.8 M H_2O ($G_{Total}(NO_3^\bullet)$ = 3.2 × 10^{-7} mol J^{-1}). This yield arises from both the direct radiolytic effect on HNO_3 and the ultrafast indirect effect of energy transfer—*via* excitation and ionization—from TBP and H_2O to HNO_3, which act as the primary precursors of $NO_3^\bullet$. Replacement of part of TBP by dodecane has little influence because they behave similarly. Despite the complexity of the system, the partial dose absorbed by each component is used to unravel the mechanism of $NO_3^\bullet$ formation and yields corresponding to direct and indirect effects across the range of concentrations studied. Interestingly, at highest HNO_3 concentration the absorbance and yield of $NO_3^\bullet$ is lower. At longer time within a few hundred nanoseconds, the decay of the $NO_3^\bullet$ radical follows pseudo-first-order kinetics and it is attributed to a hydrogen-atom transfer from TBP and dodecane to $NO_3^\bullet$. But the rate constant of this reaction is very low (0.9 × 10^6 L mol^{-1} s^{-1}) and, if the spent fuel were present, the oxidation by $NO_3^\bullet$ of uranium and plutonium ions would be expected to be predominant.

Received 4th December 2025,
Accepted 2nd March 2026

DOI: 10.1039/d5cp04724b

rsc.li/pccp

Introduction

The PUREX process is the cornerstone of modern nuclear fuel reprocessing, designed to recover valuable fissile materials, primarily uranium and plutonium, from spent nuclear fuel. This process operates in a highly complex chemical environment, further complicated by the intense internal irradiation from radionuclides, which introduces unique physical chemistry challenges.[1,2]

A critical component of the PUREX process is nitric acid (HNO_3), which serves two essential functions: it dissolves the spent fuel and regulates the redox potential of the solution; and also plays a pivotal role in separation chemistry by facilitating the formation of extractable neutral complexes, such as U(VI) ($UO_2(NO_3)_2$) and Pu(IV) ($Pu(NO_3)_4$). Tri-*n*-butyl phosphate (TBP), used as an extractant diluted in alkane at 30% (vol), is particularly effective because it can extract these neutral complexes, as well as molecular nitric acid and water, into the organic phase. The PUREX process efficiently separates uranium and plutonium from the fission products generated during nuclear reactions.[3] However, its defining characteristic is that all reactions occur simultaneously with intense auto-radiolysis of the medium, driven by the highly radioactive elements present.

The spent nuclear fuel being radioactive, the solvent used for the extraction of uranium and plutonium during the PUREX process is subjected to some radiolytic degradation. Consequently, the irradiation impact on nitric acid and TBP solutions not only challenges the stability and effective performance of the PUREX process, but also underscores the need to control radiolytic effects to ensure efficient nuclear fuel reprocessing.

Understanding how radiation affects these chemical systems is crucial for optimizing the PUREX process and ensuring the long-term sustainability of nuclear fuel management. The amplitude and mechanism of such degradation have been investigated separately on each component of the medium. Previous pulse radiolysis studies have examined the influence

[a] *Institut de Chimie Physique, UMR 8000 CNRS, Université Paris-Saclay, Bâtiment 349, Rue Magat, 91405 Orsay, France.*
E-mail: amel.zorai@universite-paris-saclay.fr
[b] *CEA, DES, ISEC, DMRC, Université de Montpellier, Bagnols-sur-Ceze 30207, France*

of radiation on either neat nitric acid or TBP separately. That was for the first time, the formation of the nitrate radical $NO_3^{\bullet}$ was observed using picosecond pulse radiolysis of concentrated aqueous nitric acid solutions.[4–9] The radical yield was found to vary with acid concentration, suggesting that both direct ionization and indirect formation by positive hole $H_2O^{+\bullet}$ trapping by NO_3^- contribute to the radical formation during the electron pulse. Subsequent studies confirmed that $NO_3^{\bullet}$ formation in aqueous nitric acid under ionizing radiation is primarily driven by direct effects and rapid electron transfer, with additional contributions from $OH^{\bullet}$ radical reactions over longer timescales and at elevated temperature.[10,11] Investigations into the ultrafast radiolytic behavior of neat TBP identified key transient species, such as the TBP-solvated electron (e^-_{TBP}) and the triplet excited state (^{3}TBP*).[12] Another study emphasized that water molecules preferentially solvate and stabilize excess electrons, potentially influencing electron-induced dealkylation during actinide separation.[13]

However, the behavior of the nitrate radical in the TBP or TBP/dodecane organic phases remains unexplored. This study aims to investigate the formation and decay of $NO_3^{\bullet}$, whose properties are expected to significantly influence the extraction reactions of uranium and plutonium in the PUREX process. The aim of this study is to determine, despite the complexity of the environment containing undissociated nitric acid, TBP, dodecane and water, the relative contributions of direct and indirect radiation effects leading to the formation of $NO_3^{\bullet}$. Notably, the solutions used here are close models of the PUREX environment, but they are free of radioactive elements and therefore autoradiolysis is not expected. Instead, the solutions are irradiated using an external picosecond electron beam source.

Experimental methods

Preparation of mixtures

The properties of HNO_3 are: MW = 63 g mol^{-1} (neat HNO_3 concentration = 15.68 M), ρ_{HNO_3} = 1.4 g mL^{-1}, pK_a = −1.37, of TBP ($C_{12}H_{27}PO_4$) are: MW = 266 g mol^{-1}, ρ_{TBP} = 0.972 g mL^{-1}, with a dielectric constant around 9 at 25 °C, and of dodecane ($C_{12}H_{26}$) are: MW = 170.3 g mol^{-1}, $\rho_{(C_{12}H_{26})}$ = 0.745 g mL^{-1}, dielectric constant ≈ 3.[14] TBP and dodecane are slightly polar solvents. High-purity TBP (≥99%) and dodecane (≥99%) were purchased from Sigma Aldrich. Nitric acid (>69%) was purchased from Fischer Scientific. Two protocols were applied to prepare series of nitric acid solutions similar to the organic phase immediately after extraction as used in the PUREX process, one with TBP, the other one with TBP and dodecane.

Series 1. Using the liquid–liquid extraction method, a volume of 100 mL of TBP was brought into contact with 100 mL of deionized water at room temperature. An identical procedure was followed for contacting 100 mL of TBP with 100 mL of nitric acid (>69%), TBP immediately turned to yellow (Fig. SI 1) due to the formation of nitrogen dioxide (NO_2) and mostly dibutyl phosphate (HDBP) and monobutylphosphate (H_2MBP).[15–17]

These procedures were repeated three times to ensure complete contact between TBP and both water and nitric acid. The organic TBP solutions obtained after this separation (corresponding to the PUREX extraction) were used for subsequent dilutions. Six organic solutions with various nitric acid concentrations [HNO_3] were prepared, in particular at 4.5 M that is intermediate in the range of 3–6 M used in the PUREX process. The final water concentration [H_2O] was at 0.8 or 1.5 M. These concentrations were based on findings from the referenced paper.[18] The final concentrations of the different reagents are summarized in Table SI 1. Only a very small part of nitric acid is dissociated into NO_3^- nitrate and H_3O^+, because of the low TBP and dodecane dielectric constants and of the low water concentration.

Series 2 involves diluting TBP in an organic solvent, with dodecane selected for this purpose. A 100 mL sample of TBP was contacted with 100 mL of nitric acid. The extracted solution was then combined with varying amounts of pure TBP and dodecane. Dodecane was chosen as the organic diluent due to its inert nature and compatibility with TBP in the PUREX process. As a hydrocarbon, dodecane is chemically stable, non-reactive with nitric acid or TBP, and crucially, it remains unreactive under irradiation.[19] Additionally, its low polarity ensures that it efficiently separates the aqueous and organic phases without interfering with the extraction process. This allows for better control over the distribution of nitric acid and TBP, enabling accurate adjustments in concentration and facilitating the study of extraction dynamics.[20] Water and nitric acid concentrations were maintained constant.

The concentration of nitric acid was determined according to the previously described method, and that of water by using the Karl Fischer coulometric titration.[18] That of TBP without dodecane was obtained from the complementary volume or with dodecane from initial amounts before extraction.

Pulse radiolysis measurements

Ultra-short electron pulses with a typical width of 5–10 ps are produced by the ELYSE platform based on excitation of a CsTe photocathode using a femtosecond laser pulses at the frequency of 5 Hz.[21,22]

The sample optical cells, made of synthetic fused silica, have optical path length l = 0.5 cm. They have 200 μm thick optical windows to minimize contributions from transient species generated in the quartz cell by the electron beam.

For picosecond pump–probe experiments using optical absorption, the broad band from 355 to 750 nm is generated by focusing part of the fundamental laser beam into a CaF_2 crystal, and is split 60/40 into probe and reference paths. Both beams are coupled into optical fibers and sent to a spectrometer for analysis using a cooled CCD camera.

For the detection of the optical absorption signals of transient species in the picosecond to microsecond range, the probe beam is provided by a home-made repetitive lamp and analyzed by a streak camera. The signal absorbances measured may be as low as a few %.

The reference dose D_w was determined from the absorbance at 640 nm of the hydrated electron in neat water.[22] The doses

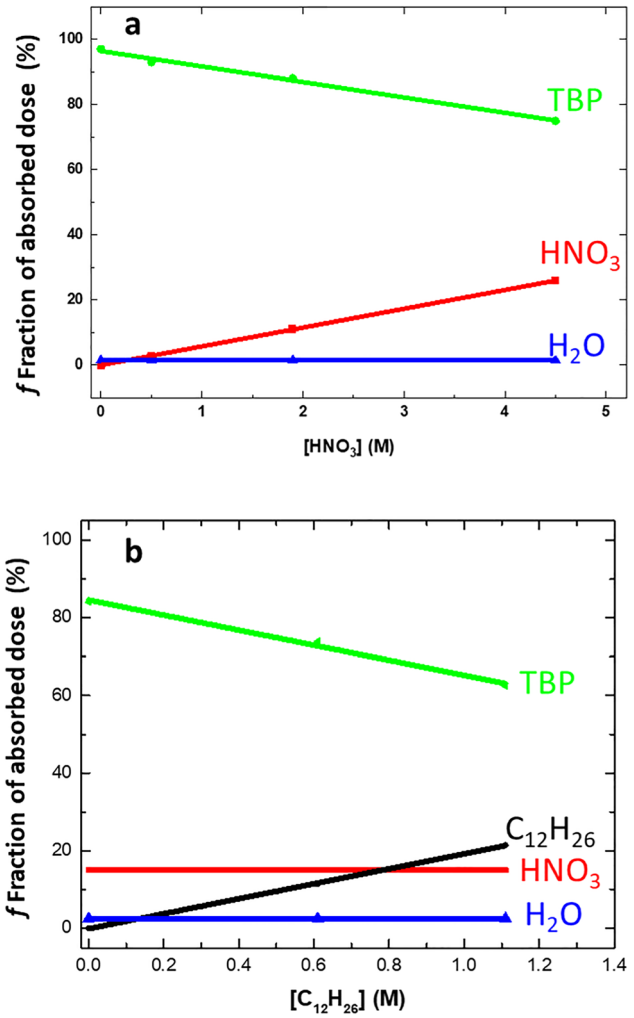

Fig. 1 (a) Dependence of fractions f of the total doses absorbed by each component TBP, HNO_3 or H_2O on the HNO_3 concentration in the environment without dodecane. (b) Dependence of fractions f of the total doses absorbed by the components on the dodecane concentration ($[HNO_3]$ = 2.5 M and $[H_2O]$ = 1.5 M are constant).

absorbed by each component of HNO_3/TBP/H_2O/$C_{12}H_{26}$ solutions were calculated by considering their specific electronic density (Tables SI 1 and SI 3). The calculated doses (in J L^{-1}) absorbed by HNO_3, TBP, H_2O, $C_{12}H_{26}$, and the corresponding dose fractions f of the total dose are given for the various dose fractions f of the total dose are given for the various concentrations in Fig. 1(a), (b), and Tables SI 1 and SI 3 according to the following equations:

$$f(HNO_3) = \text{Dose}(HNO_3)/\text{Total dose} \quad (1)$$

$$f(HNO_3) + f(TBP) + f(H_2O) + f(C_{12}H_{26}) = 1 \quad (2)$$

Results and discussions

The spectra-kinetics data constitute a large matrix of data for the absorbance at different times and at different wavelengths. The experiments have been twice repeated. Remarkably, despite the low values of the measured absorbances, the uncertainty on their average values is less than ±5%.

The time-evolution of the transient optical absorption spectra is presented in Fig. 2 for the HNO_3 concentrations of 0.5, 1.9, and 4.5 M.

In solution containing 4.5 M HNO_3, the band with peaks at 640 and 670 nm (Fig. 2(c)) correspond fairly well to the radical $NO_3^{\bullet}$. However, a very weak absorbance of another species is also observed around 440 nm.

The initial spectra at 5 ps for 0.5 and 1.9 M HNO_3 (Fig. 2(a) and (b)) are more complex because around 640 nm the shape differs from the radical $NO_3^{\bullet}$ spectrum. Additionally, an absorption band is also observed around 440 nm and another one in the range 700–780 nm, increases to the near infrared where the $NO_3^{\bullet}$ radical does not absorb (Fig. 2). It is assigned to e^-_{TBP}.[12]

Fig. 3 presents the kinetics at the wavelengths 440, 640 and 780 nm for the medium with 1.9 M HNO_3/3.3 M TBP/0.8 M H_2O. Clearly, the rate differences in the decays at these wavelengths (Fig. 3) indicate that three distinct species are early induced by the ultra-short pulse. Note that in neat TBP (HNO_3 free)[12] the observed transient spectra are initially constituted of the very intense e^-_{TBP} spectrum ($\varepsilon(e^-_{TBP})_{780nm}$ = 9800 L mol^{-1} cm^{-1}).[12] It overlaps the much weaker band of the longer lived excited state TBP* which is observed alone only in the nanosecond range.

In 0.5 and 1.9 M HNO_3 solutions, the band present in near infrared, where $NO_3^{\bullet}$ does not absorb, is thus assigned to the electron solvate in TBP as the major component, e^-_{TBP}. The absorbance around 640 nm, typically observed in 4.5 M HNO_3 environment is assigned to $NO_3^{\bullet}$.

The 440 nm band, though absorbing in the same range as the less intense one observed in neat TBP,[12] belongs to a different species which will be discussed further.

Note that the e^-_{solv} spectrum extends also in the visible range down to 400 nm and that it overlaps both other bands.

Primary radiation effects on the components

The radiation energy absorbed within the pulse by the electrons of the molecules constituting the mixture is responsible for the species formation. The major part of it is absorbed by the TBP. However, some fraction is also directly absorbed by the other components HNO_3 and H_2O, proportionally to their electronic density that increases with their concentration (Fig. 1 and Table SI 1). Therefore, the four components of the medium are directly excited and ionized by their irradiation partial dose, as in neat nitric acid,[11] TBP,[12] water,[23] and dodecane:[14]

$$HNO_3 \rightsquigarrow HNO_3^{\bullet}, HNO_3^{+\bullet} + e^- \quad (3)$$

$$TBP \rightsquigarrow TBP^*, TBP^{+\bullet} + e^- \quad (4)$$

Note that in neat TBP (HNO_3 free) the observed transient spectra are initially constituted of the very intense e^-_{TBP} spectrum ($\varepsilon(e^-_{TBP})_{780nm}$ = 9800 L mol^{-1} cm^{-1}).[12] It overlaps the much weak band of the longer-lived excited state TBP* which is observed alone only in the nanosecond range.

$$H_2O \rightsquigarrow H_2O^*, H_2O^{+\bullet} + e^- \quad (5)$$

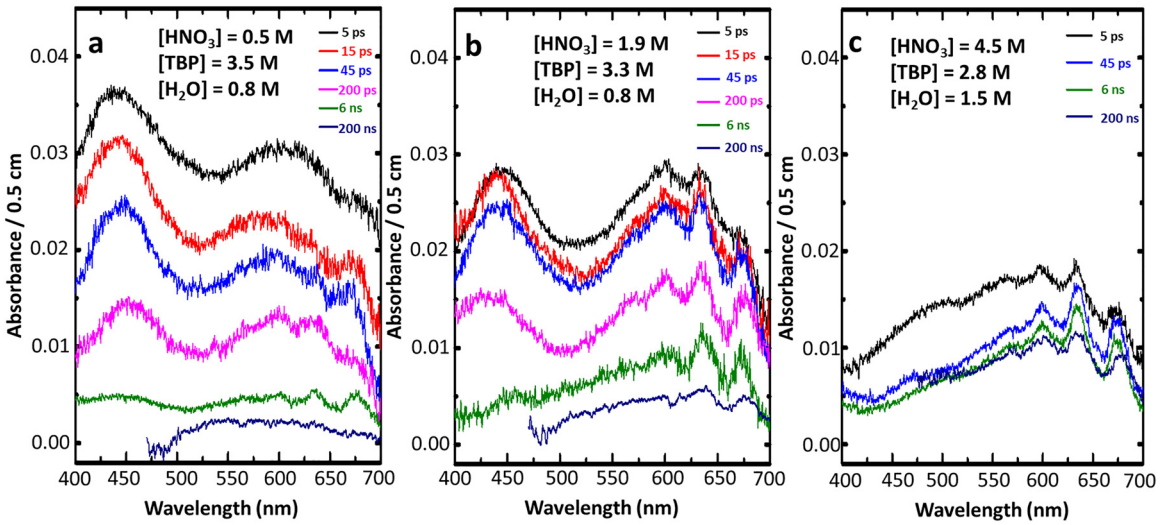

Fig. 2 Time evolution since 5 ps of transient optical absorption spectra of irradiated organic media. (a) 0.5 M HNO_3/3.5 M TBP/0.8 M H_2O. (b) 1.9 M HNO_3/3.3 M TB/0.8 M H_2O. (c) 4.5 M HNO_3/2.7 M TBP/1.5 M H_2O. Dose per pulse is D_w = 100 Gy and Optical path l = 0.5 cm.

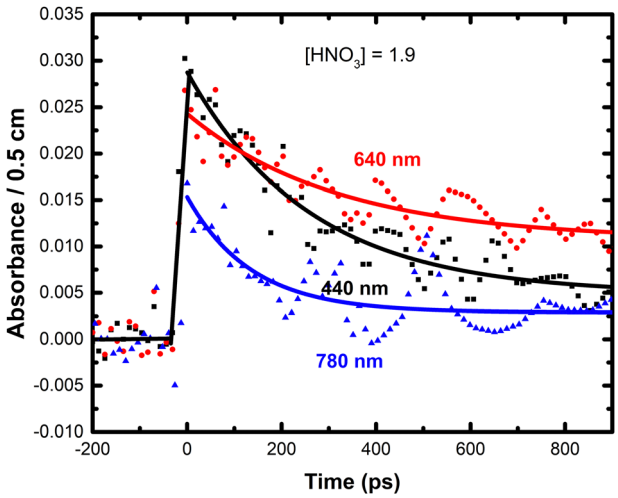

Fig. 3 Kinetics at 440, 640, 780 nm for 1.9 M HNO_3/3.3 M TBP/0.8 M H_2O. Dose per pulse is D_w = 100 Gy. Optical path l = 0.5 cm.

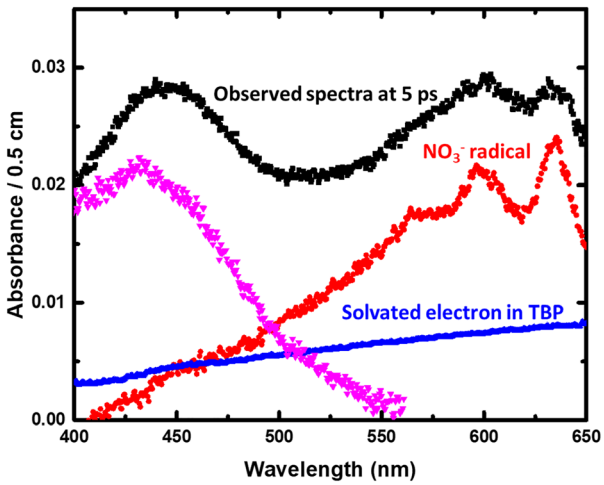

Fig. 4 Deconvolution of the observed spectrum at 5 ps for solution containing 1.9 M HNO_3 (Fig. 2) into the transient spectra of e^-_{TBP}, $NO_3^\bullet$ and the 440 nm band, in the range of 400 to 650 nm. Optical path l = 0.5 cm.

$$C_{12}H_{26} \rightsquigarrow C_{12}H_{26}{}^{*}, C_{12}H_{26}{}^{+\bullet} + e^- \quad (6)$$

$$e^- \rightarrow e^-_{solv} \quad (7)$$

Deconvolution of the optical absorption spectrum at 5 ps

The spectral shape/intensity of the early radiation-induced short-lived species in the solutions with 0.5 and 1.9 M HNO_3, must be first quantitatively separated in order to allow their shape and yield determination.

In solutions either with 0.5 and 1.9 M HNO_3, the absorbances due to e^-_{TBP}, $A(e^-_{TBP})_{5ps}$, are obtained at 780 nm (where it alone absorbs), from initial values in kinetics (Fig. 3 and Table SI 2). Then the corresponding partial absorbances of e^-_{TBP} at 640 and 440 nm are derived from its known absorption spectrum,[12] normalized at the 780 nm values (Table SI 2). The absorbances of the other band at 440 and 640 nm are obtained separately by subtraction of $A(e^-_{TBP})_{5ps}$ from the measured total absorbances (Table SI 2).

A complete and quantitative deconvolution of the measured spectrum at 5 ps for the 1.9 M HNO_3 solution is presented in Fig. 4. The e^-_{TBP} spectrum is obtained by a normalization of the published spectrum at $A(e^-_{TBP})_{5ps,780nm}$ = 0.012 (Table SI 2 and Fig. 4). The $NO_3^\bullet$ spectrum is determined *via* the normalization at the maximum value of $A(NO_3^\bullet)_{5ps,640nm} = A_{Total,5ps,640nm} - A(e^-_{TBP})_{5ps,640nm}$ = 0.0213 (Table SI 2 and Table 1, Fig. 4).

Finally, the 440 nm band is obtained from the difference between the overall measured spectrum and those of e^-_{TBP} and of the $NO_3^\bullet$ radical (Fig. 4). The end-of-pulse absorbance values at 440 nm are given in Table SI 2. Note that the maximum wavelength of the total absorbance is slightly shifted in time from 440 to 450 nm when the part due to e^-_{solv} vanishes.

Table 1 Dependence on the HNO_3, TBP, H_2O concentrations (dose fraction f) of the $NO_3^\bullet$ absorbance at 640 nm (0.5 cm) and yields arising from irradiation direct and indirect effects

$[HNO_3]$ (M), (f)	0.5, (0.029)	1.9, (0.11)	4.5, (0.25)
[TBP] (M), (f)	3.5, (0.955)	3.3, (0.875)	2.84, (0.726)
$[H_2O]$ (M), (f)	0.8, (0.015)	0.8, (0.015)	1.5, (0.025)
A_{780} (e^-)$_{TBP}$ (0.5 cm), at 5 ps	0.017	0.012	0
$G(e^-)_{TBP}$ (10^{-7} mol J^{-1}) at 5 ps	0.35	0.24	0
$A_{640}(NO_3^\bullet)$ (0.5 cm) at 5 ps	0.016	00213	0.018
$G(NO_3^\bullet)_{Total}$ (10^{-7} mol J^{-1}) at 5 ps	2.47	3.2	2.7
$G(NO_3^\bullet)_{Direct}$ (10^{-7} mol J^{-1}) at 5 ps	3.4	3.4	3.4
$A_{640}(NO_3^\bullet)$ Direct effect at 5 ps	0.00064	0.00247	0.0058
$A_{640}(NO_3^\bullet)$ Indirect effect at 5 ps	0.0154	0.0189	0.0122
$G(NO_3^\bullet)_{Indirect}$ (10^{-7} mol J^{-1}) at 5 ps	2.4	3.17	2.46

Though all three spectra overlap, particularly that of e^-_{TBP} in the whole visible domain, the spectra of the 640 and 440 nm bands do not overlap each other at their respective maxima.

The radiolytic initial yield $G(e^-_{TBP}) = A(e^-_{TBP})_{5ps,780nm}/(l \times \varepsilon(e^-_{TBP}) \times \text{Dose})$ is very low and decreases from 0.35×10^{-7} mol J^{-1} at 0.5 M HNO_3 to 0.24×10^{-7} mol J^{-1} at 1.9 M HNO_3 and 0 at 4.5 M HNO_3 (Fig. 3 and Table 1), as compared to the value of 1.6×10^{-7} mol J^{-1} at 5 ps in neat TBP.[12] In fact, the reactions of solvated electrons with HNO_3/NO_3^- are very fast and e^-_{solv} is mostly scavenged within the pulse:

$$e^-_{solv} + HNO_3\ (NO_3^-) \rightarrow HNO_3^{-\bullet}(NO_3^{2-\bullet}) \quad (8)$$

Radical $NO_3^\bullet$ yields

The $NO_3^\bullet$ absorbance values at 5 ps and 640 nm $A_{640}(NO_3^\bullet) = A_{640}(\text{measured}) - A_{640}(e^-_{TBP})$ (Table SI 2 and Fig. 4) and the corresponding concentrations (with ε_{640} = 1350 L mol^{-1} cm^{-1} and ε_{670} = 1080 L mol^{-1} cm^{-1})[8] are given in Table 1.

The specific formation processes of the radical $NO_3^\bullet$ result in part from the direct-effect of the radiation absorption by HNO_3 (reaction (1)) and the fast dissociation of HNO_3* and $HNO_3^{+\bullet}$ (reactions (9)–(11)), that are expected to increase proportionally to the partial dose absorbed by HNO_3 or ($NO_3^\bullet$) (Table SI 1):

$$HNO_3^* \rightarrow NO_3^\bullet + H^\bullet \quad (9)$$

A small part of HNO_3* may be decomposed also:

$$HNO_3^* \rightarrow NO_2 + {}^\bullet O^\bullet \quad (10)$$

$$HNO_3^{+\bullet} \rightarrow NO_3^\bullet + H^+ \quad (11)$$

However, the part of the dose $f(HNO_3)$ directly absorbed by HNO_3 in reaction (3), proportionally to its concentration (Table SI 1 and Fig. 1(a)) is too small to account alone for the $NO_3^\bullet$ absorbance values observed at 5 ps as given in Fig. 4 and Table 1.

Each component of the medium also absorbs directly radiation depending on its electron fraction (Fig. 1 and Table SI 1). The primary species concentrations are proportional to these fractions f. The $NO_3^\bullet$ radical may be also induced by the ultrafast excitation energy or charge transfer from the primary radiolytic species of the other components, *i.e.* TBP and H_2O induced by the respective partial dose (Table SI 1) as indirect effects.

$$HNO_3 + TBP^* \rightarrow HNO_3^* + TBP \rightarrow NO_3^\bullet + H^\bullet + TBP \quad (12)$$

$$HNO_3 + TBP^{+\bullet} \rightarrow HNO_3^{+\bullet} + TBP \rightarrow NO_3^\bullet + H^+ + TBP \quad (13)$$

In presence of dodecane, similar transfers occur:

$$HNO_3 + C_{12}H_{26}^* \rightarrow HNO_3^* + C_{12}H_{26} \rightarrow NO_3^\bullet + H^\bullet + C_{12}H_{26} \quad (14)$$

$$HNO_3 + C_{12}H_{26}^{+\bullet} \rightarrow HNO_3^{+\bullet} + C_{12}H_{26} \rightarrow NO_3^\bullet + H^+ + C_{12}H_{26} \quad (15)$$

Though the contribution of H_2O, factor $f(H_2O)$, is almost negligible, according to the radiolysis study of concentrated aqueous solutions of HNO_3 (TBP free),[24] it has been demonstrated that the excitation energy absorbed by H_2O is also transferred to HNO_3:

$$HNO_3 + H_2O^* \rightarrow HNO_3^* + H_2O \rightarrow NO_3^\bullet + H^\bullet + H_2O \quad (16)$$

Moreover, in these solutions,[11] the $NO_3^\bullet$ radical is indirectly produced after the pulse by H atom transfer from HNO_3 to the radical $OH^\bullet$ issued from the reactions (15) and (16):

$$H_2O^{+\bullet} + H_2O \rightarrow OH^\bullet + H_3O^+ \quad (17)$$

$$HNO_3 + OH^\bullet \rightarrow NO_3^\bullet + H_2O \quad (18)$$

This slower process is not observed in presence of TBP, suggesting that the $OH^\bullet$ radical is rapidly scavenged by TBP as the predominant component:

$$TBP + OH^\bullet \rightarrow TBP(-H)^\bullet + H_2O \quad (19)$$

The total yield $G_{Total}(NO_3^\bullet)$ for the various environments are obtained (Table 1) as the ratios between the values of the $[NO_3^\bullet]$ concentration and the total dose absorbed by allotment the components (Table SI 1). It is an overall value including direct and indirect effects, characterized by specific yields (Table 1):

$$G(NO_3^\bullet)_{Total} = f(NO_3^\bullet) \times G(NO_3^\bullet)_{Direct} + f(TBP) \times G(NO_3^\bullet)_{Indirect\ TBP} + f(C_{12}H_{26}) \times G(NO_3^\bullet)_{Indirect\ C_{12}H_{26}} + f(H_2O) \times G(NO_3^\bullet)_{Indirect\ H_2O} \quad (20)$$

However, the dose fraction $f(H_2O)$ is very small ($\leq$1.5%) (Tables SI 1 and SI 3) and processes involving water species are negligible.

We may first remark that the value of $G_{Total}(NO_3^\bullet) = 3.2 \times 10^{-7}$ mol J^{-1} for the intermediate concentration 1.9 M HNO_3 is the largest (Table 1). An excitation yield is certainly involved to account for the measured yield. Considering the opposite variations of the doses absorbed by HNO_3 and TBP (Fig. 1(a)), the sum of the direct and indirect effects is the most favored for the medium 1.9 M HNO_3/3.3 M TBP. The solvated electron yield $G(e^-_{solv}) = 0.35$ and 0.24×10^{-7} mol J^{-1} at 5 ps, for 0.5 and 1.9 M HNO_3 respectively, is obtained (Table 1) with $\varepsilon(e^-_{TBP})_{780nm}$ = 9800 L mol^{-1} cm^{-1}.[12] The values are much lower than 1.6×10^{-7} mol J^{-1} at 7 ps in neat TBP,[12] or than the ionization yields in polar liquid,[25] because the solvated electrons are scavenged by the nitric acid.

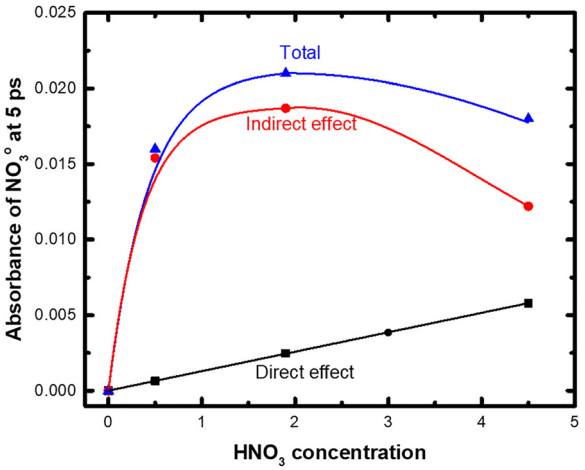

Fig. 5 Dependence on the HNO_3 concentration of the total $NO_3^\bullet$ absorbance measured at 640 nm, and of the calculated partial absorbances by direct and indirect effects. Optical path l = 0.5 cm (Table 1).

Direct effects

The parts of direct and indirect effects have been already evaluated separately in highly concentrated aqueous HNO_3 solutions and in neat HNO_3.[11] The $NO_3^\bullet$ yield of direct effects of excitation and ionization on neat HNO_3 is $G(NO_3^\bullet) = 3.4 \times 10^{-7}$ mol J^{-1},[11] and the same value is taken for HNO_3 in TBP solutions (Table 1). The corresponding absorbances are proportional to the partial dose absorbed by HNO_3 (Table 1 and Fig. 5).

Indirect effects

Note that the indirect effects yields $G(NO_3^\bullet)_{Indirect}$ in Table 1 are relative to the effects together from TBP and H_2O radiolytic species. The absorbances $A_{640}(NO_3^\bullet)_{Indirect}$ are obtained from the difference $A_{640}(NO_3^\bullet)_{Total} - A_{640}(NO_3^\bullet)_{Direct}$ (Table 1 and Fig. 5).

Contrarily to $G(NO_3^\bullet)_{Direct}$, the yields $G(NO_3^\bullet)_{Indirect}$ are not constant and do depend on the medium composition. The yields of indirect effects on HNO_3 arise first from irradiation reactions (4) and (5) of TBP or H_2O with a constant yield. But these reactions are followed by partial transfer *via* reactions (12) and (13) with a ratio depending on competitive processes in the medium. Namely, the yield $G(NO_3^\bullet)_{Indirect}$ increases between $[HNO_3]$ = 0.5 and 1.9 M because of the increasing competition of the transfer reaction (13) much favored than the reaction (19):

$$TBP^{+\bullet} + TBP \rightarrow TBP + TBP(-H)^\bullet + H^+ \quad (21)$$

Despite the HNO_3 concentration increase by a 3.8 factor between 0.5 and 1.9 M, the yield increase is only from 2.4 to 3.17×10^{-7} mol J^{-1} (Table 1), and we may consider that the transfer is almost complete in 1.9 M solution.

However, in 4.5 M HNO_3/2.8 M TBP/1.5 M H_2O, the indirect yield decrease drastically down to $G(NO_3^\bullet)_{Indirect} = 2.46 \times 10^{-7}$ mol J^{-1} (Table 1). At this high HNO_3 concentration, not only e^-_{solv} is totally scavenged by HNO_3 (reaction (8)), but also a part of its presolvated precursor e^- is scavenged:

$$e^- + HNO_3(NO_3^-) \rightarrow HNO_3^{-\bullet}(NO_3^-)^- \quad (22)$$

Reaction (22) is favored by the high value of the ratio 4.5 M HNO_3/2.8 M TBP. This reaction of electron attachment on HNO_3 (NO_3^-) is in competition[25] with reaction (7) of electron solvation in TBP and with reaction (21) inducing the formation of part of the singlet excited state $^1TBP^*$:

$$e^- + TBP^{+\bullet} \rightarrow {}^1TBP^* \quad (23)$$

Thus, part of $^1TBP^*$ as precursor of $NO_3^\bullet$ *via* reaction (12) is lost. Actually, the cations $TBP^{+\bullet}$ escaping from the recombination (23) are less efficient than $^1TBP^*$ to induce $NO_3^\bullet$ because the ionization transfer (13) is itself in competition with a partial transfer towards TBP (reaction (21)) or H_2O *via* reaction (24), so depleting the $G(NO_3^\bullet)_{Indirect}$ yield between 1.9 and 4.5 M HNO_3:

$$H_2O + TBP^{\bullet+} \rightarrow H_2O^{+\bullet} + TBP \quad (24)$$

Note that, when comparing these results in TBP solutions with those in similar highly concentrated HNO_3 solutions in water,[11] the indirect yield is indeed much lower in water because reactions (18) and (24) inhibit the formation of the $NO_3^\bullet$ radical.

Species absorbing at 440 nm

No absorbance such as the absorption band at 440 nm, arising at the end-of-pulse in the HNO_3/TBP/H_2O environment (Fig. 2(a) and (b)), was observed in aqueous HNO_3 solutions.[11] In neat TBP (HNO_3 free), a much weaker and longer-lived band was observed at almost the same wavelength and was assigned to an excited state of TBP.[12] The same assignment cannot be excluded, provided assuming the huge differences in intensity and stability behavior were just the consequence of the strong acidity of the present environment.

The value of this initial absorbance is decreasing when $[HNO_3]$ is increased from 0.5 to 1.9 M, and becoming negligible at 4.5 M (or when in parallel [TBP] decreases from 3.5 to 2.7 M). Moreover, the 440 nm absorbance decreases when, at constant HNO_3 concentration, that of TBP is reduced by its partial replacement by dodecane (Table SI 2 and Fig. SI 2). Seemingly, the formation of the species absorbing at 440 nm requires an early crossed reaction during both HNO_3 and TBP radiolysis.

Time-evolution of the transient species absorbance ($t > 5$ ps)

As shown in Fig. 3, the absorbance intensity decay kinetics depend on the wavelength, therefore on the short-lived species.

At 780 nm, the e^-_{TBP} absorbance is alone and decays to 0 within 200 ps *via* reaction (5) (Fig. 6(b)).

At 680 nm, in 0.5 and 1.9 M solutions, the fast absorbance decay of e^-_{TBP} during 200 ps is superimposed to the decay of the $NO_3^\bullet$ absorbance which is very slow (Fig. 6(a)).

However, in the 4.5 M solution (Fig. 6(a)), where no solvated electron is detected at 780 nm, the very small initial decay at 640 nm must be assigned to some intra-spur reaction of $NO_3^\bullet$.

After 200 ps, when the interference of the e^-_{TBP} absorbance is over, the $NO_3^\bullet$ absorbance at 640 nm decreases slowly to zero by a pseudo first-order process (Fig. 7). It is worthy to note that the decay rate decreases markedly in 4.5 M HNO_3 compared to the concentrations 0.5 or 1.9 M. On the contrary, it increases

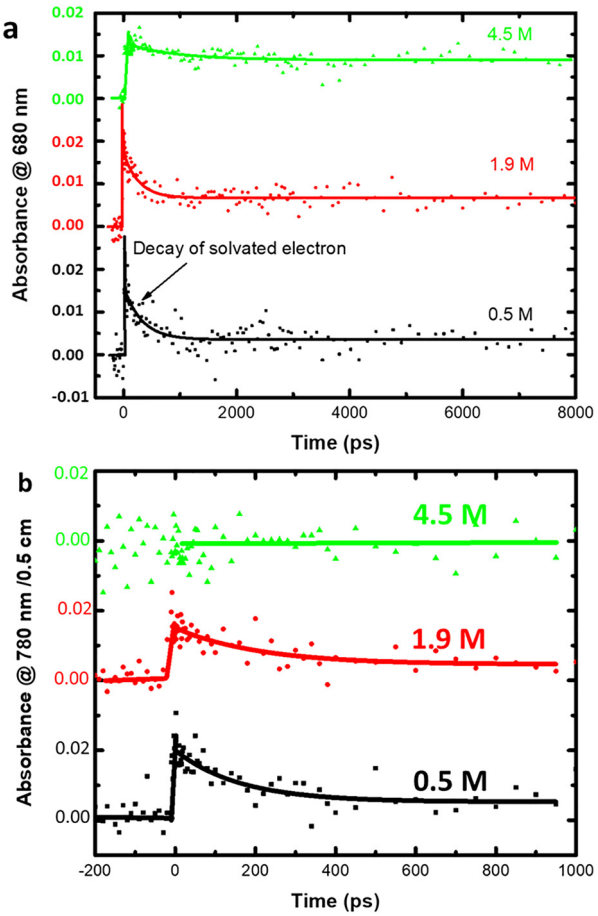

Fig. 6 Compared absorbance decays for various HNO_3 concentrations at (a) 680 nm, (b) 780 nm.

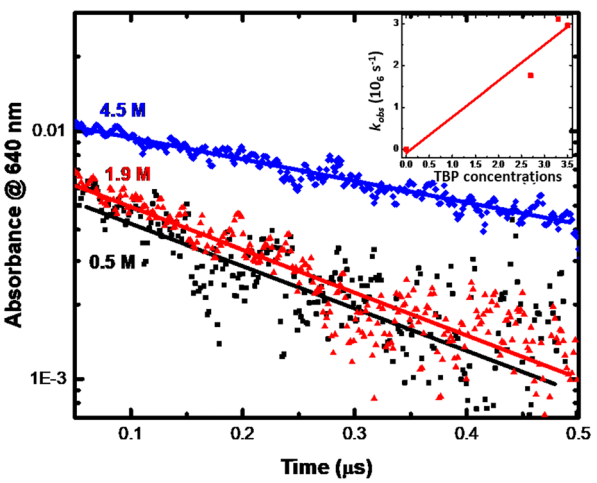

Fig. 7 Pseudo first-order decay of the 640 nm absorbance at various HNO_3 concentrations. Inset: dependence of the pseudo-first order rate constant on the TBP concentration.

proportionally to the corresponding TBP concentration as shown in Fig. 7, inset. This suggests a reaction of the radical $NO_3^\bullet$ with TBP:

$$NO_3^\bullet + TBP \rightarrow HNO_3 + TBP(-H)^\bullet \quad (25)$$

From the slope of the linear dependence of the pseudo first-order rate constant on the TBP concentration (Fig. 7, Inset), the bimolecular rate constant is $k_{21} = 0.9 \times 10^6$ L mol^{-1} s^{-1}. The value of this rate constant is much lower than the diffusion controlled one, as expected for H transfer reactions.

During the PUREX process, the above environment is irradiated by the spent nuclear fuel, which is dissolved by the nitric acid, and the ions of uranium and plutonium are selectively extracted *via* complexation by nitrate anion and solvation by TBP/$C_{12}H_{26}$. As the reaction rate constant between $NO_3^\bullet$ and U^{IV} was measured in water as $k(U^{IV} + NO_3^\bullet) = 1.6 \times 10^6$ L mol^{-1} s^{-1},[2] it is expected that the complexed ions of uranium and plutonium are then oxidized to U^{VI} and Pu^{VI}, respectively, either directly by $NO_3^\bullet$ radicals, in competition with reaction (22), or by TBP(–H)$^\bullet$ and $C_{12}H_{25}^\bullet$ radicals arising from this reaction. The oxidation yield is that of $NO_3^\bullet$ and is the highest for the environment 1.9 M HNO_3/3.3 M TBP/0.8 M H_2O ($G_{Total}(NO_3^\bullet)$ = 3.2×10^{-7} mol J^{-1}). Note that in these oxidation reactions the solvents HNO_3 and TBP are restored. Eventually, the reduction balance by electrons is supported by HNO_3 only.

The absorbance at 440 nm beyond 200 ps decreases according to a first order reaction (Fig. 8). The rates are very close each other and independent of the HNO_3 concentration at 0.5 and 1.9 M.

Influence of dodecane

In order to determine the influence of dodecane compared with TBP, data were obtained in replacing part of TBP ($C_{12}H_{27}PO_4$) volumes by dodecane ($C_{12}H_{26}$). The total dose slightly decreases at increasing dodecane concentration (from 0 to 1.1 M) because of its lower electronic density (Table SI 3, Fig. 1(b)). The $NO_3^\bullet$ absorbances and yields at 50 ns (e^-_{TBP} has vanished) are given in Table 2. At constant HNO_3 and H_2O concentrations, the $NO_3^\bullet$ yields with dodecane are lower than without. Seemingly, the energy transfer to HNO_3 is less efficient from irradiated dodecane than from TBP (reactions (12)–(15)).

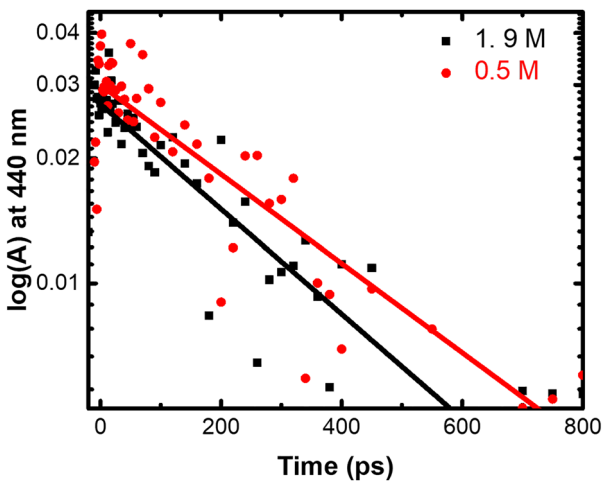

Fig. 8 First-order decay of the absorbance at 440 nm for HNO_3 concentrations 0.5 and 1.9 M.

Table 2 Dependence of the $NO_3^\bullet$ absorbances and yield on the dodecane concentrations

$[C_{12}H_{26}]$ (M), (f)	0, (0)	0.61, (0.11)	1.11, (0.215)
[TBP] (M), (f)	3.1, (0.84)	2.6, (0.72)	2.2, (0.624)
$[HNO_3]$ (M), (f)	2.5, (0.15)	2.5, (0.15)	2.5, (0.16)
$[H_2O]$ (M), (f)	1.5, (0.025)	1.5, (0.025)	1.5, (0.025)
$A(NO_3^\bullet)_{Total,640nm,50ns}$ 0.5 cm	0.007	0.005	0.004
Dose (Total) (J L^{-1})	100.3	96.5	94
$G(NO_3^\bullet)_{Total,50ns}$ (10^{-7} mol J^{-1})	1.0	0.78	0.63

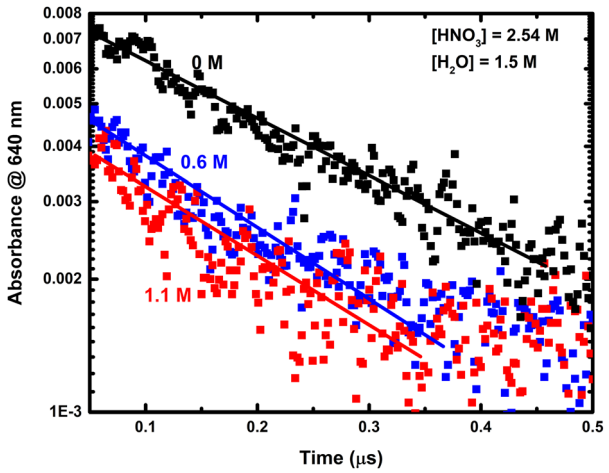

Fig. 9 Dependence on the TBP and dodecane concentrations in HNO_3 2.5 M/H_2O 1.5 M environments (Table 2) of the kinetics of the $NO_3^\bullet$ radical absorbance at 640 nm in logarithmic scale. Optical path 0.5 cm.

The influence of dodecane on the decay of the $NO_3^\bullet$ radical absorbance at 640 nm is shown in Fig. 9.

The decays are compared for the same HNO_3 2.5 M and H_2O 1.5 M concentrations, but variable TBP/$C_{12}H_{26}$ environments ($[C_{12}H_{26}]$ from 0 to 1.1 M). At any time, the absorbances with dodecane are lower than without. However, clearly, the decays in presence of TBP/dodecane are pseudo-first order as without dodecane. Moreover, the slope is very slightly increasing as much as does the sum: [TBP] + $[C_{12}H_{26}]$. That indicates that dodecane and TBP behave similarly and with the same bimolecular rate constant in the oxidation reactions (25) and (26) by $NO_3^\bullet$:

$$NO_3^\bullet + C_{12}H_{26} \rightarrow HNO_3 + C_{12}H_{25}^\bullet \qquad (26)$$

The $C_{12}H_{25}^\bullet$ radical is expected as well as $NO_3^\bullet$ and TBP(–H)$^\bullet$ to oxidize U^{IV} and Pu^{IV} during the PUREX process.

Conclusions

Using picosecond pulse radiolysis, the transient optical absorption spectra were thoroughly PUREX model environments with various HNO_3/TBP/H_2O/$C_{12}H_{26}$ fractions. The optical absorption spectra at the end of the pulse (5 ps) are composed of the overlapping absorption band around 440 nm, hypothetically assigned to some acidic form of a TBP excited state, a band with specific peaks around 640 nm, assigned to the $NO_3^\bullet$ radical, and a broad spectrum from 400 to the near infrared that is assigned to e^-_{TBP}, the electron solvated in TBP. The observed overall spectrum has been deconvoluted into the separate spectra of the short-lived species. The e^-_{TBP} decay is extremely rapid *via* the reaction with HNO_3 within the pulse and the yield at 5 ps is very low.

The HNO_3 and TBP/dodecane concentrations and doses absorbed change with opposite trends, but the total $NO_3^\bullet$ radical yield at 5 ps has the highest value for the 1.9 M HNO_3/3.3 M TBP/0.8 M H_2O environment ($G_{Total}(NO_3^\bullet)$ = 3.2×10^{-7} mol J^{-1}). The radical $NO_3^\bullet$ is early induced both *via* direct excitation and ionization of HNO_3, and indirectly *via* the transfer of energies absorbed by TBP/$C_{12}H_{26}$/H_2O to HNO_3. Despite the complexity of the environment, the mechanism and separate absorbances and yields of these direct and indirect radiation effects are determined and discussed.

The absorbance of the $NO_3^\bullet$ radical decreases with time by a bimolecular reaction with TBP and dodecane. However, the rate constant is very low ($k = 0.9 \times 10^6$ L mol^{-1} s^{-1}). In the PUREX process where the environment is irradiated by the spent nuclear fuel, the ions of uranium and plutonium complexed by TBP are oxidized to U^{VI} and Pu^{VI} either directly by the early induced $NO_3^\bullet$ radical or by the further TBP(–H)$^\bullet$/$C_{12}H_{25}^\bullet$ radicals induced by $NO_3^\bullet$, the most efficiency being observed for the environment 1.9 M HNO_3/3.3 M TBP/0.8 M H_2O. Its degradation is mostly supported by HNO_3 which is reduced *via* electrons scavenging.

Author contributions

AZ, MB, and SD performed the experiments with the support of DA. Calculations were done by MM and DA. The manuscript was written by JB, MM, AZ, PM, DA and finalized through the contributions of all authors. All authors have given approval to the final version of the manuscript.

Conflicts of interest

There are no conflicts to declare.

Note added after first publication

This article replaces the original version published on 18th March 2026 which contained an error in eqn (10). The remainder of the article remains unchanged.

Data availability

A data availability statement (DAS) is required to be submitted alongside all articles.

Supplementary information (SI) includes the optical absorption spectra of neat TBP and of various solutions of nitric acid; a table showing the dependence of the dose absorbed by the mixture components on their concentration; and a table showing the how the absorbances and yields of e^-_{TBP} and radical were obtained. See DOI: https://doi.org/10.1039/d5cp04724b.

Acknowledgements

This work was supported by CNRS through the NEEDS program and CNRS grant on RadConNOP. The authors deeply thank Jean-Philippe Larbre and Denis Dobrovolskii for their help during the picosecond pulse radiolysis experiments at ELYSE.

Notes and references

1 R. P. Wayne, I. Barnes, P. Biggs, J. P. Burrows, C. E. Canosa-Mas, J. Hjorth, G. Le Bras, G. K. Moortgat, D. Perner, G. Poulet, G. Restelli and H. Sidebottom, The nitrate radical: Physics, chemistry, and the atmosphere, *Atmos. Environ.*, 1991, **25**, 1–203.

2 M. A. H. Khan, M. C. Cooke, S. R. Utembe, A. T. Archibald, R. G. Derwent, P. Xiao, C. J. Percival, M. E. Jenkin, W. C. Morris and D. E. Shallcross, Global modeling of the nitrate radical (NO_3) for present and pre-industrial scenarios, *Atmos. Res.*, 2015, **164–165**, 347–357.

3 A. R. Kazanjian, F. J. Miner, A. K. Brown, P. G. Hagan and J. W. Berry, Radiolysis of nitric acid solution: L.E.T. effects, *Trans. Faraday Soc.*, 1970, **66**, 2192–2198.

4 M. Daniels, Radiation chemistry of the aqueous nitrate system. III. Pulse electron radiolysis of concentrated sodium nitrate solutions, *J. Phys. Chem.*, 1969, **73**, 3710–3717.

5 R. K. Broszkiewicz, The radiation-induced formation of NO_3 in aqueous solutions, *Int. J. Appl. Radiat. Isot.*, 1967, **18**, 25–32.

6 P. K. Bhattacharyya and R. D. Saini, Radiolytic yields G(HNO_2) and G(H2O2) in the aqueous nitric acid system, *Int. J. Radiat. Phys. Chem.*, 1973, **5**, 91–99.

7 T. Loegager and K. Sehested, Formation and decay of peroxynitrous acid: a pulse radiolysis study, *J. Phys. Chem.*, 1993, **97**, 6664–6669.

8 Y. Katsumura, P. Y. Jiang, R. Nagaishi, T. Oishi, K. Ishigure and Y. Yoshida, Pulse radiolysis study of aqueous nitric acid solutions: formation mechanism, yield, and reactivity of NO_3 radical, *J. Phys. Chem.*, 1991, **95**, 4435–4439.

9 G. Garaix, G. P. Horne, L. Venault, P. Moisy, S. M. Pimblott, J. Marignier and M. Mostafavi, Decay Mechanism of $NO_3^\bullet$ Radical in Highly Concentrated Nitrate and Nitric Acidic Solutions in the Absence and Presence of Hydrazine, *J. Phys. Chem. B*, 2016, **120**, 5008–5014.

10 A. Balcerzyk, A. K. El Omar, U. Schmidhammer, P. Pernot and M. Mostafavi, Picosecond Pulse Radiolysis Study of Highly Concentrated Nitric Acid Solutions: Formation Mechanism of $NO_3^\bullet$ Radical, *J. Phys. Chem. A*, 2012, **116**, 7302–7307.

11 R. Musat, S. A. Denisov, J.-L. Marignier and M. Mostafavi, Decoding the Three-Pronged Mechanism of $NO_3^\bullet$ Radical Formation in HNO_3 Solutions at 22 and 80 °C Using Picosecond Pulse Radiolysis, *J. Phys. Chem. B*, 2018, **122**, 2121–2129.

12 F. Wang, G. P. Horne, P. Pernot, P. Archirel and M. Mostafavi, Picosecond Pulse Radiolysis Study on the Radiation-Induced Reactions in Neat Tributyl Phosphate, *J. Phys. Chem. B*, 2018, **122**, 7134–7142.

13 T. Bahry, S. A. Denisov, P. Moisy, J. Ma and M. Mostafavi, Real-Time Observation of Solvation Dynamics of Electron in Actinide Extraction Binary Solutions of Water and *n*-Tributyl Phosphate, *J. Phys. Chem. B*, 2021, **125**, 3843–3849.

14 Y. Yoshida, T. Ueda, T. Kobayashi, H. Shibata and S. Tagawa, Studies of geminate ion recombination and formation of excited states in liquid *n*-dodecane by means of a new picosecond pulse radiolysis system, *Nucl. Instrum. Methods Phys. Res., Sect. A*, 1993, **327**, 41–43.

15 L. K. Patil, V. G. Gaikar, S. Kumar, U. K. Mudali and R. Natarajan, Thermal Decomposition of Nitrated Tri-*n*-Butyl Phosphate in a Flow Reactor, *Int. Sch. Res. Notices*, 2012, **2012**, 193862.

16 A. Dodi and G. Verda, Improved determination of tributyl phosphate degradation products (mono- and dibutyl phosphates) by ion chromatography, *J. Chromatogr. A*, 2001, **920**, 275–281.

17 V. S. Smitha, J. S. V. Kumar, M. Surianarayanan, H. Seshadri and N. V. Lakshman, Reactive chemical pathway of tributyl phosphate with nitric acid, *Process Saf. Envion. Prot.*, 2018, **116**, 677–684.

18 B. Mokili and C. Poitrenaud, Modelling of Nitric Acid and Water Extraction From aqueous Solutions Containing a Salting-Out Agent by Tri-N-Butylphosphate, *Solvent Extr. Ion Exch.*, 1995, **13**, 731–754.

19 J. P. Holland, J. F. Merklin and J. Razvi, The radiolysis of dodecane-tributylphosphate solutions, *Nucl. Instrum. Methods Phys.*, 1978, **153**, 589–593.

20 I. Billard, Are molecular solvents, aqueous biphasic systems and deep eutectic solvents meaningful categories for liquid–liquid extraction?, *C. R. Chim.*, 2022, **25**, 67–81.

21 J. Belloni, H. Monard, F. Gobert, J.-P. Larbre, A. Demarque, V. De Waele, I. Lampre, J.-L. Marignier, M. Mostafavi, J. C. Bourdon, M. Bernard, H. Borie, T. Garvey, B. Jacquemard, B. Leblond, P. Lepercq, M. Omeich, M. Roch, J. Rodier and R. Roux, ELYSE—A picosecond electron accelerator for pulse radiolysis research, *Nucl. Instrum. Methods Phys. Res., Sect. A*, 2005, **539**, 527–539.

22 J.-L. Marignier, V. de Waele, H. Monard, F. Gobert, J.-P. Larbre, A. Demarque, M. Mostafavi and J. Belloni, Time-resolved spectroscopy at the picosecond laser-triggered electron accelerator ELYSE, *Radiat. Phys. Chem.*, 2006, **75**, 1024–1033.

23 G. V. Buxton, C. L. Greenstock, W. P. Helman and A. B. Ross, Critical Review of rate constants for reactions of hydrated electrons, hydrogen atoms and hydroxyl radicals ($^\bullet OH/^\bullet O^-$) in Aqueous Solution, *J. Phys. Chem. Ref. Data*, 1988, **17**, 513–886.

24 S. J. Kruse, S. K. Scherrer, G. P. Horne, J. A. LaVerne and T. Z. Forbes, The inorganic chemist's guide to actinide radiation chemistry: a review, *Inorg. Chem. Front.*, 2025, **12**, 6398–6434.

25 J. Belloni and J. L. Marignier, Electron-solvent interaction: attachment solvation competition, *Int. J. Radiat. Appl. Instrum., Part C*, 1989, **34**, 157–171.